PAPER

Gyrofluid potential vorticity equation and turbulent equipartion states

To cite this article: J Madsen *et al* 2015 *Plasma Phys. Control. Fusion* **57** 054016

View the article online for updates and enhancements.

Related content

- Zonal flows and pattern formation
  Ö D Gürcan and P H Diamond

- The influence of temperature dynamics and dynamic finite ion Larmor radius effects on seeded high amplitude plasma blobs
  M. Held, M. Wiesenberger, J. Madsen et al.

- Pinch effect in two-dimensional turbulence
  J Nycander and J Juul Rasmussen

Recent citations

- Angular momentum and rotational energy of mean flows in toroidal magnetic fields
  M. Wiesenberger and M. Held

- Collisional transport across the magnetic field in drift-fluid models
  J. Madsen *et al*

- 25 Years of Self-organized Criticality: Space and Laboratory Plasmas
  A. Surjalal Sharma *et al*

Corrigendum: 'Gyrofluid potential vorticity equation and turbulent equipartion states' (2015 *Plasma Phys. Control. Fusion* 57 054016)

J Madsen, J Juul Rasmussen, V Naulin, A H Nielsen and F Treue

Department of Physics, Technical University of Denmark, DK-2800 Kgs. Lyngby, Denmark

E-mail: jmad@fysik.dtu.dk

CrossMark

This corrigendum corrects two misprints in the published paper. The results presented in the published paper are correct and are not affected by the misprints. The authors sincerely regret the mistakes. We thank Markus Held (University of Innsbruck) for pointing out the misprints in equation (2).

In the ion gyro-center pressure equation (equation (2) in the original paper) two terms describing finite Larmor radius corrections to the $\boldsymbol{E} \times \boldsymbol{B}$-drift are missing. The terms include the drift velocity

$$\boldsymbol{u}_2 = \frac{\hat{\boldsymbol{b}} \times \nabla \Gamma_2 \phi}{B}. \tag{1}$$

The correct form of the ion gyro-center equation reads

$$\frac{\partial}{\partial t} P_{i\perp} + \nabla \cdot \left(P_{i\perp}[\boldsymbol{u}_E + 2\boldsymbol{u}_T + 2\boldsymbol{u}_\eta + \boldsymbol{u}_2] \right) \\ - P_{i\perp}(\boldsymbol{u}_E + 2\boldsymbol{u}_\eta + \boldsymbol{u}_2) \cdot \nabla \ln B = 0. \tag{2}$$

Furthermore, on the left-hand side of equation (21) in the original paper N_i should be replaced by $P_{i\perp}$. The correct form of equation (21) is

$$\nabla \cdot (P_{i\perp} \boldsymbol{u}_\eta) = \nabla \cdot (P_{i\perp} \boldsymbol{u}_\Omega) + N_i \Gamma_2 \phi \nabla T_{i\perp} \cdot \frac{\hat{\boldsymbol{b}} \times \nabla \ln B}{B} \\ - \nabla T_{i\perp} \cdot \frac{\hat{\boldsymbol{b}} \times \nabla (N \Gamma_2 \phi)}{B}. \tag{3}$$

1

Gyrofluid potential vorticity equation and turbulent equipartion states

J Madsen, J Juul Rasmussen, V Naulin, A H Nielsen and F Treue

Department of Physics, Technical University of Denmark, DK-2800 Kgs. Lyngby, Denmark

E-mail: jmad@fysik.dtu.dk

CrossMark

Abstract

An equation governing potential vorticity in a magnetized plasmas is derived. The equation is analogous to Ertel's theorem. In the long wave-length limit the potential vorticity equals the ratio of the gyro-frequency plus the $\boldsymbol{E} \times \boldsymbol{B}$- and diamagnetic polarization densities to the particle density. The equation is relevant for transport barriers in magnetically confined plasmas because particle density, ion temperature and the radial electric field are mutually coupled through the potential vorticity. The potential vorticity equation is derived from an energy conserving, four-field, electrostatic, full-F gyrofluid model. It is shown that the gyrofluid model possesses two exact Lagrangian invariants. In systems where mixing uniformly distribute the Lagrangian invariants we derive the corresponding turbulent equipartion states. It is shown that the system is driven towards constant potential vorticity. Given particle density and magnetic field profiles we infer ion temperature and electric potential profiles from the derived turbulent equipartion states.

Keywords: gyrofluid, potential vorticity, turbulent equipartion, zonal flows, transport barriers

(Some figures may appear in colour only in the online journal)

1. Introduction

The concept of potential vorticity (PV) dates back to Ertel's theorem [1] which governs the time-evolution of PV. The theorem is an invaluable aid in understanding large scale fluid flows, particularly in planetary [2] and astrophysical fluid dynamics [3]. Analogues to Ertel's theorem in plasma physics exist [4, 5], but they have not had the same impact as Ertel's theorem. For ideal neutral fluids, PV is a Lagrangian invariant, i.e. it is conserved by each fluid element along its trajectory and hence puts strong constraints on the dynamic evolution of the fluid. Highly relevant for magnetically confined plasmas are the applications of Ertel's theorem to systems with zonal flows in geophysical [2, 6–8] and astrophysical fluid dynamics [3]. By zonal flows we mean sheared banded flows. A prominent example [3] is the banded cloud pattern and east-west directed jets in the atmosphere of Jupiter. Common for these systems with zonal flows is the appearance of mixing in combination with non-constant PV profiles. In the context of PV dynamics, zonal flows are understood as a consequence of a stepwise homogenization of PV, forming a PV staircase.

Each step forms a region of approximately constant PV and the zonal flows are strongest in the vicinity of the interfaces between these regions of constant PV.

Similar ideas have been explored in plasma physics, where in particular turbulent equipartion (TEP) theory has been used to explain the formation of non-collisional density and temperature profiles and the associated pinch velocities [9–14]. In these theories Lagrangian invariants are mixed in regions bounded by closed streamlines. If the mixing is sufficiently strong, the existence of a small collisional diffusion homogenizes the Lagrangian invariants making them constant in the bounded regions. Turbulent equipartion theory has also been used to derive toroidal [15] and poloidal [16] momentum profiles and associated pinch velocities.

Here, we derive an equation analogues to Ertel's theorem governing the time-evolution of the magnetic-field-aligned PV from a full-F, electrostatic, 2D slab, collisionless gyrofluid model. In the long wave-length limit the PV reads

$$\Pi \simeq \frac{\Omega_i + \omega^*}{n_i},$$

where ω^* contains the magnetic-field-aligned $E \times B$ and dia-magnetic vorticity, n_i is the particle density and Ω_i is the ion gyro-frequency. Further, we identify two Lagrangian invariants of the model and derive two TEP states of the system. Interestingly, the first TEP state drives the system towards constant ∏. Finally, we discuss the coupling between the radial electric field and the ion pressure prescribed by the TEP profile, in relation to zonal flows and transport barriers in magnetically confined plasmas and analogies to PV stair-cases in geophysical and astrophysical fluid dynamics.

The remainder of the paper is organized as follows. In section 2 we present the full-F gyrofluid model used in this paper. A PV equation is presented in section 3. In section 4 TEP states and the associated profiles are presented. In section 5 we discuss the results in relation to transport barrier physics. Finally, we sum up the results in section 6.

2. Model

In this work we shall adopt a gyrofluid model [17] derived from full-F gyrokinetic [18] equations. Since we address the interplay between low-frequency turbulence and profiles, the full-F gyrofluid model is a good choice because it is global in the sense that no distinctions between fluctuations and back-ground profiles are made. The model is fully non-linear and hence can describe micro-turbulence with gradient length-scales comparable to the gyro-radius. Furthermore, for alge-braic manipulation gyrofluid models have an advantage over other low-frequency fluid models [19, 20] because the *gyro-viscous cancellations* [21, 22] appear naturally. In gyrofluid models the cancellation is carried out at the gyrokinetic level, which implies relatively simple gyrofluid model equations. The simplicity of gyrofluid models is striking because FLR-corrected drift fluid models can be recovered from gyrofluid models [17, 23–25].

Here, we restrict our analysis to a simple, electrostatic plasma in a 2D slab perpendicular to the magnetic field. Collisions and dynamics parallel to the magnetic field are neglected. Ions are described by the gyro-center density N_i and the perpendicular gyro-center pressure $P_{i\perp}$, whose time-evolutions are governed by

$$\frac{\partial}{\partial t} N_i + \nabla \cdot \left(N_i[\boldsymbol{u}_E + \boldsymbol{u}_T + \boldsymbol{u}_\eta]\right) = 0, \tag{1}$$

$$\frac{\partial}{\partial t} P_{i\perp} + \nabla \cdot \left(P_{i\perp}[\boldsymbol{u}_E + 2\boldsymbol{u}_T + 2\boldsymbol{u}_\eta]\right)$$
$$- P_{i\perp}(\boldsymbol{u}_E + 2\boldsymbol{u}_\eta) \cdot \nabla \ln B = 0, \tag{2}$$

where the ion gyrofluid velocities are

$$\boldsymbol{u}_E = \frac{\hat{\boldsymbol{b}} \times \nabla \psi}{B}, \quad \boldsymbol{u}_T = T_{i\perp} \frac{\hat{\boldsymbol{b}} \times \nabla \ln B}{q_i B}, \quad \boldsymbol{u}_\eta = \Gamma_2 \phi \frac{\hat{\boldsymbol{b}} \times \nabla \eta}{B}. \tag{3}$$

The perpendicular gyro-center temperature is defined as $T_{i\perp} = P_{i\perp}/N_i$ and B denotes the magnetic field strength. The generalized potential

$$\psi = \Gamma_1 \phi - \frac{m \mid \nabla_\perp \phi \mid^2}{2 q_i B^2}, \tag{4}$$

entering the $E \times B$-drift $\boldsymbol{u}_E$ includes the gyro-averaged electro-static potential $\Gamma_1 \phi$ and the $E \times B$-energy which is important for momentum and energy conservation. The gyro-average operator $\Gamma_1 = 1 + \rho^2/2\nabla_\perp^2 + \cdots$, is the gyrofluid moment of the gyrokinetic gyro-averaging operator, where $\rho^2 = T_{i\perp}/(m_i\Omega_i^2)$ is the non-constant, thermal gyro-radius. $\boldsymbol{u}_T$ is the gyrofluid representation of the ∇B-drift and $\boldsymbol{u}_\eta$ describes corrections to the gyro-averaged electric potential by the second gyro-average operator $\Gamma_2 = T_\perp \frac{\partial \Gamma_1}{\partial T_\perp}$ due to spatial variations of tem-perature and magnetic field strength $\nabla \eta = \nabla \ln B - \nabla \ln T_{i\perp}$.

As a consequence of the smallness of the electron to ion mass ratio, only the lowest order terms in the electron gyro-center coordinate transformation are retained, which corre-sponds to neglect of electron finite Larmor radius and finite electron inertia effects. Therefore, the electron gyrofluid moment variables are identical to the corresponding fluid moment variables e.g. $N_e = n_e$. The electron equations are

$$\frac{\partial}{\partial t} n_e + \nabla \cdot \left(n_e[\boldsymbol{v}_E + \boldsymbol{v}_T]\right) = 0, \tag{5}$$

$$\frac{\partial}{\partial t} p_{e\perp} + \nabla \cdot \left(p_{e\perp}[\boldsymbol{v}_E + 2\boldsymbol{v}_t]\right) - p_{e\perp}\boldsymbol{v}_E \cdot \nabla \ln B = 0, \tag{6}$$

where

$$\boldsymbol{v}_E = \frac{\hat{\boldsymbol{b}} \times \nabla \phi}{B}, \tag{7}$$

$$\boldsymbol{v}_t = -t_{e\perp} \frac{\hat{\boldsymbol{b}} \times \nabla \ln B}{eB}, \tag{8}$$

are the electron $E \times B$-drift and ∇B-drift, respectively and the perpendicular electron temperature is $t_{e\perp} = p_{e\perp}/n_e$. In passing we note that the diamagnetic cancellations in equations (1) and (2) appeared automatically. In order to emphasize the fun-damental difference between particle and gyrofluid moments, all standard particle fluid moments are written in lower case letters (e.g. n_i, n_e, p_i, p_e, $t_{i\perp}$, $t_{e\perp}$) whereas gyrofluid moments are written in upper case letters (e.g. N_i, $P_{i\perp}$, $T_{i\perp}$).

Electrons and ions are coupled through the quasi-neutrality constraint. By expressing the ion particle density n_i in terms of gyrofluid moment variables we get

$$n_e = n_i = \Gamma_1^\dagger N_i + \nabla \cdot \left(\frac{N_i}{\Omega_i B} \nabla_\perp \phi\right). \tag{9}$$

The operator $\Gamma_1^\dagger = 1 + \nabla_\perp^2 \rho^2/2 + \cdots$ is the Hermitian conjugate operator to Γ_1. Note that the Laplacian in $\Gamma_1^\dagger$ operates on ρ^2. This equation is also referred to as the *polarization equation* due to the explicit appearance of the polarization density, the last term on the right hand side, which is the manifestation of the polarization drift in gyrokinetic models [18] or equiva-lently the divergence of the polarization drift current [24–26] in drift fluid models.

The total conserved energy for this system is

$$\mathcal{E} = \int \mathrm{d}^3\boldsymbol{r} \left(\frac{m_i N_i \, | \, \nabla_\perp \phi|^2}{2B^2} + P_{i\perp} + p_{e\perp} \right), \qquad (10)$$

where boundary terms were discarded.

3. Potential vorticity equation

In neutral fluid dynamics Ertel's theorem [1] is an indispensable aid, particularly in geophysical and planetary fluids, for comprehension of the character and physics of a wide range of phenomena. By combining the fluid vorticity and density equations we get an equation

$$\frac{\mathrm{d}}{\mathrm{d}t}\Pi = \frac{\boldsymbol{\omega}}{n} \cdot \nabla S + \nabla\lambda \cdot \frac{\nabla n \times \nabla p}{n^3} + \frac{\nabla\lambda}{n} \cdot \nabla \times \frac{\boldsymbol{F}}{n} \quad (11)$$

describing the time evolution of PV: $\Pi = \boldsymbol{\omega} \cdot \nabla\lambda/n$. Here, n denotes the neutral fluid density, $\boldsymbol{\omega} = \nabla \times \boldsymbol{u}$ is the vorticity associated with the velocity field $\boldsymbol{u}$, $\mathrm{d}/\mathrm{d}t = \partial/\partial t + \boldsymbol{u} \cdot \nabla$ is the material derivative, $\boldsymbol{F}$ is the frictional force and λ is some scalar satisfying

$$\frac{\mathrm{d}\lambda}{\mathrm{d}t} = S,$$

where S is a source. Ertels theorem states that *if*: (i) λ is a conserved quantity, (ii) the fluid is either barotropic (i.e. the baroclinic vector vanishes: $\nabla n \times \nabla p = 0$) or if λ is solely a function of n and p and (iii) the friction force F is negligible, *then* PV is a Lagrangian invariant, i.e. conserved in the frame moving with the velocity $\boldsymbol{u}$.

For a system steadily rotating with angular velocity Ω the PV becomes $\Pi = (2\,\Omega + \boldsymbol{\omega}_r) \cdot \nabla\lambda/n$, where $\boldsymbol{\omega}_r$ is the relative vorticity measured in the rotating frame of reference.

To demonstrate the power of the concept of PV, we consider an example from oceanography. Large-scale flows in the ocean are well described by shallow water models [2]. Furthermore, frictional forces are negligible and the fluid is nearly barotropic. Therefore, any conserved fluid scalar λ implies conservation of a corresponding potential vorticity. Since vertical mixing of the water column is negligible, the relative position of a fluid parcel $\lambda = (z - h_B)/H$ over the ocean bottom at h_B in a fluid column of height H is a Lagrangian invariant which implies that

$$\frac{\mathrm{d}}{\mathrm{d}t}\frac{f + \omega_r}{Hn} = 0$$

is a Lagrangian invariant. $f = 2\Omega \sin\theta$ is the Coriolis parameter describing the component of the planetary vorticity 2Ω normal to the ocean surface at latitude $\theta (f = 0$ at equator). Since the density n can be considered constant PV conservation tightly couples the local vorticity of the water column ω_r, the height H and the local component of the planetary vorticity f. Phenomena such as the spin-up of water columns when moving from shallow to deeper water and the path of the Gulf stream through the Atlantic Ocean can be explained by the concept of PV conservation in shallow water models.

Here we will show that the ion gyro-center density equation (1) provides an analogy to Ertel's theorem. For low ion temperature a plasma fluid analogue is readily derived from

the ion equations of motion showing that $(\Omega_i + \boldsymbol{\omega})/n$ is conserved in the inviscid limit when the baroclinic contribution vanishes [4]. Our work considers the case of non-zero ion temperature. In order to obtain the gyrofluid PV equation we introduce the following drifts

$$\boldsymbol{u}_\Omega = T_{i\perp} \frac{\hat{\boldsymbol{b}} \times \nabla(\frac{N\Gamma_2\phi}{T_{i\perp}})}{N_i B}, \qquad \boldsymbol{u}_D = \frac{\hat{\boldsymbol{b}} \times \nabla P_{i\perp}}{qN_i B}. \quad (12)$$

The divergences of the corresponding fluxes equal the original terms in equation (1)

$$\nabla \cdot (N_i \boldsymbol{u}_T) = \nabla \cdot (N_i \boldsymbol{u}_D), \qquad \nabla \cdot (N_i \boldsymbol{u}_\eta) = \nabla \cdot (N_i \boldsymbol{u}_\Omega). \quad (13)$$

Using these relations the gyro-center density equation (1) can be recast as

$$\frac{\mathrm{d}^*}{\mathrm{d}t}\ln\left(\frac{\Omega_i}{N_i}\right) = \hat{\boldsymbol{b}} \cdot \frac{\nabla \ln \frac{N_i}{T_{i\perp}} \times \nabla T^*}{qB}, \qquad (14)$$

where we have defined the material derivative and the modified temperature

$$\frac{\mathrm{d}^*}{\mathrm{d}t} = \frac{\partial}{\partial t} + [\boldsymbol{u}_E + \boldsymbol{u}_D + \boldsymbol{u}_\Omega] \cdot \nabla, \qquad T^* = T_\perp + q\Gamma_2\phi, \quad (15)$$

respectively. To see that equation (14) in fact describes the time-evolution of PV we express the ion gyro-center density N_i in terms of particle density n_i, perpendicular pressure $p_{i\perp}$ and the electrostatic potential ϕ by solving equation (9) for N_i. In the long wavelength limit (LWL) $k_\perp^4 \rho^4 \ll 1$, where $k_\perp$ is the typical inverse perpendicular gradient length scale, we obtain the following expression for the gyro-center density

$$N_i \simeq n_i(1 - \frac{\omega^*}{\Omega_i}), \qquad (16)$$

where

$$\omega^* = \frac{\Omega_i}{n_i}[\nabla_\perp^2(\frac{p_{i\perp}}{2m\Omega_i^2}) + \nabla \cdot \left(\frac{n_i}{B\Omega_i}\nabla_\perp\phi\right)]. \qquad (17)$$

The last term in equation (17) equals the component of the $\boldsymbol{E} \times \boldsymbol{B}$-drift vorticity $\hat{\boldsymbol{b}} \cdot \nabla \times \boldsymbol{u}_E = \nabla \cdot (B^{-1}\nabla_\perp\phi)$ aligned with the magnetic field plus a cross-term $\nabla\ln(n_i/\Omega_i) \cdot \nabla_\perp \phi/B$. The first term in equation (17) equals half the magnetic-field-aligned component of the diamagnetic vorticity $1/2\hat{\boldsymbol{b}} \cdot \nabla \times \boldsymbol{u}_D = 1/2\nabla \cdot (\nabla_\perp p_i/(qn_iB))$ plus a cross-term $1/2 (qn_iB)^{-1}\nabla_\perp p_i \cdot [\nabla\ln n_i + 3\nabla\Omega_i]$. Only half the diamagnetic vorticity appears which is a consequence of the underlying gyro-viscous cancellation which to lowest order annihilates the diamagnetic advection of momentum and thereby breaks the symmetry in the inertia term. Since ω^*/Ω_i is small:

$$\frac{\Omega_i}{N_i} \simeq \frac{\Omega_i + \omega^*}{n_i} \qquad (18)$$

and hence equation (14) becomes

$$\frac{\mathrm{d}^*}{\mathrm{d}t}\ln\left(\frac{\Omega_i + \omega^*}{n_i}\right) = \hat{\boldsymbol{b}} \cdot \frac{\nabla \ln \frac{N_i}{T_{i\perp}} \times \nabla T^*}{qB}. \qquad (19)$$

Identifying $\hat{\boldsymbol{b}}$ as $\nabla\lambda$ we note the strong resemblance of this equation to Ertel's equation (11).

To sum up, the electrostatic, 2D slab geometry gyrofluid PV equation (14) implies that in regions where (i) viscous forces, external forces and parallel dynamics can be neglected and (ii) when the right hand side—the modified baroclinic vector—vanishes, Ω_i/N is a Lagrangian invariant. This PV theorem is important for, e.g. zonal flow generation because it links the electric field to the density and temperature profiles through equation (16). We will discuss this further in section 5.

4. Lagrangian invariants and turbulent equipartition profiles

We will now identify two quantities that are conserved along specific fluid trajectories. These Lagrangian invariants are derived by combining the gyrofluid PV equation (14) with a recasted version of the perpendicular gyro-center pressure equation (2). First, we use the identities

$$\nabla \cdot (P_{i\perp}\boldsymbol{u}_T) = \nabla \cdot (P_{i\perp}\boldsymbol{u}_D) + P_{i\perp}\nabla T_{i\perp} \cdot \frac{\hat{\boldsymbol{b}} \times \nabla \ln B}{qB}$$
$$- \nabla T_{i\perp} \cdot \frac{\hat{\boldsymbol{b}} \times \nabla P_{i\perp}}{qB}, \qquad (20)$$

$$\nabla \cdot (N_i\boldsymbol{u}_\eta) = \nabla \cdot (P_{i\perp}\boldsymbol{u}_\Omega) + N_i\Gamma_2\phi\nabla T_{i\perp} \cdot \frac{\hat{\boldsymbol{b}} \times \nabla \ln B}{B}$$
$$- \nabla T_{i\perp} \cdot \frac{\hat{\boldsymbol{b}} \times \nabla(N\Gamma_2\phi)}{B}, \qquad (21)$$

to write equation (2) as

$$\frac{d^*}{dt}\ln\frac{P_{i\perp}}{N_i^2} = -2\frac{\hat{\boldsymbol{b}} \times \nabla T^*}{qB} \cdot \nabla\ln\frac{N_i}{B}, \qquad (22)$$

where the material derivative and the generalized temperature T^* are defined in equation (15). The symmetry of equations (14) and (22) suggests [10] the Lagrangian invariants to be on the following form:

$$\nabla L = \nabla\left[\alpha\ln\frac{N_i}{B} + \ln\frac{P_{i\perp}}{N_i^2}\right], \qquad (23)$$

where α is scalar. An equation for L is obtained by combining equations (14) and (22), which can be solved for α requiring that L is a Lagrangian invariant. Two solutions $\alpha = \pm\sqrt{2}$ are obtained corresponding to the exact Lagrangian invariants

$$\nabla L_\pm = \nabla\left[\pm\sqrt{2}\ln\frac{N_i}{B} + \ln\frac{P_{i\perp}}{N_i^2}\right], \qquad (24)$$

conserved along orbits determined by

$$\left(\frac{d^*}{dt} + \boldsymbol{u}_\pm \cdot \nabla\right)L_\pm = 0, \qquad (25)$$

where

$$\boldsymbol{u}_\pm = \pm\sqrt{2}\frac{\hat{\boldsymbol{b}} \times \nabla T_i^*}{qB}. \qquad (26)$$

The electron fluid also possesses Lagrangian invariants which can be directly derived from the governing equations (1) and (2) or alternatively by evaluating equation (25) in the limit of small gyro-radius. Either way, the electron invariants are

$$\nabla l_\pm = \nabla\left[\pm\sqrt{2}\ln\frac{n_e}{B} + \ln\frac{p_{e\perp}}{n_e^2}\right], \qquad (27)$$

which are conserved along trajectories with velocities

$$\boldsymbol{v} = \boldsymbol{v}_E - \frac{\hat{\boldsymbol{b}} \times \nabla p_{e\perp}}{en_eB} \mp \sqrt{2}\frac{\hat{\boldsymbol{b}} \times \nabla T_{e\perp}}{eB}. \qquad (28)$$

4.1. Turbulent equipartion profiles

Regardless of whether the flow is laminar or turbulent, $L_\pm$ and $l_\pm$ are Lagrangian invariants. In either case, if in a bounded region the mixing time-scale is faster than other competing time-scales (e.g. collisional diffusion time-scale), the Lagrangian invariants will be uniformly distributed, a state denoted turbulent equipartition (TEP) [9, 27]. A simple example is the equipartition of n/B in simplified 2D drift-fluid turbulence [12, 28], which implies that the particle density profile is given by the magnetic field $n \sim B$ and that n is transported up-gradient by the so-called curvature pinch velocity [27].

Here, we are concerned with mixing of the Lagrangian invariants L_+ and L_- given in equation (24). An equipartion of L_+ and L_- due to turbulent mixing implies that profiles are driven towards

$$\frac{N_i}{B} = \text{const.}, \qquad \frac{T_{i\perp}}{B} = \text{const.} \qquad (29)$$

Interestingly, the $N_i \propto B$ TEP profile drives the system towards constant PV, whose time-evolution is given in equation (14). To further investigate the TEP state, it is instructive to express the PV and therefore the ion gyro-center density in terms of measurable quantities. Since we are concerned with profiles inferred from the TEP state, we take the ion gyro-center density in the LWL as in equation (18) which allows us to express the $N_i \propto B$ TEP profile as

$$\frac{\Omega_i + \omega^*}{n_i} \simeq \text{const.} = c_1, \qquad (30)$$

where ω^* is defined in equation (17). In order to express the TEP $T_{i\perp} \propto B$ profile in terms of measurable quantities, a relation similar to the quasi-neutrality constraint equation (9) for the perpendicular ion particle pressure $p_{i\perp}$ is needed. Using the same procedures [17] which led to equation (9) we obtain the following LWL approximation for the perpendicular ion gyro-center pressure

$$P_{i\perp} = p_{i\perp} - p_i^*, \quad p_i^* = \nabla_\perp^2\left(\frac{t_{i\perp}p_{i\perp}}{m_i\Omega_i^2}\right) + 2\nabla\cdot\left(\frac{p_{i\perp}}{B\Omega_i}\nabla_\perp\phi\right), \quad (31)$$

and hence that the profiles in the LWL are driven towards

$$\frac{c_1(p_{i\perp} - p_i^*)}{B\Omega} \simeq \text{const.} = c_2, \quad (32)$$

where equation (30) was inserted.

Equations (30) and (32) form a coupled set of ordinary differential equations. For example if the particle density n and the magnetic field strength B are specified, the electric potential ϕ and the perpendicular ion temperature $t_{i\perp}$ can be determined given appropriate boundary conditions and values of the constants c_1 and c_2. The TEP states therefore couple the particle density, the ion temperature, the magnetic field and the electric field profiles. To illustrate this point we consider the special case where $\Omega/n = C$ is constant. In that situation ω^*/Ω is also constant and hence equations (30) and (32) reduce to the coupled equations

$$\frac{\mathrm{d}}{\mathrm{d}x}E = \frac{\mathrm{d}^2}{\mathrm{d}x^2}\left(\frac{t_{i\perp}}{2m_i\Omega_i}\right) - \Omega_i C(c_1 - C), \quad (33)$$

$$\frac{\mathrm{d}}{\mathrm{d}x}\left(\frac{Et_{i\perp}}{B}\right) = \frac{c_2}{2Cc_1} - \frac{t_{i\perp}\Omega_i}{2} + \frac{1}{2}\frac{\mathrm{d}^2}{\mathrm{d}x^2}\left(\frac{t_{i\perp}}{m_i\Omega_i}\right), \quad (34)$$

where $E = -\frac{\mathrm{d}}{\mathrm{d}x}\phi$ denotes the electric field and x is the 'radial' slab coordinate anti-parallel to the magnetic field gradient. In this special case the coupling of the electric field and the ion temperature is evident. We will discuss this coupling further in the next section.

Lastly, a uniform distribution of the electron fluid Lagrangian invariants l_+ and l_- due to turbulent mixing implies that the electron profiles are driven towards

$$\frac{n_e}{B} = \text{const.}, \qquad \frac{t_{e\perp}}{B} = \text{const.}, \quad (35)$$

as was also found in [27]. The result obtained here can easily be derived for isotropic electron temperature $t_{e\perp} = t_{e|}$.

We would like to emphasize that profiles predicted by TEP theory must be used with care because ions and electrons are coupled. Especially, if the ion TEP states are used to infer the electric field profile without considering the electrons, as is possible using equations (30) and (32). However, it is easily imaginable that ion and electron TEP states are not simultaneously reached, e.g. if their particle, momentum and heat sinks and sources are different. Given that the ion and electron profiles are simultaneously driven towards their corresponding TEP states, the ion profiles in equation (29) reduce to

$$\frac{1}{B}\frac{\mathrm{d}}{\mathrm{d}x}\left(\frac{E}{B}\right) = \text{const.}, \qquad \frac{t_{i\perp}}{B} + \frac{2}{B^2\Omega_i}E\frac{\mathrm{d}}{\mathrm{d}x}t_{i\perp} = \text{const.} \quad (36)$$

respectively. In this state the shearing rate of the radial electric field follows the magnetic field with a variation constrained by the ion temperature profile.

5. Discussion

In a magnetically confined fusion plasma we cannot expect PV nor the Lagrangian invariants in equations (29) and (35) to be globally mixed and hence uniformly distributed over the entire plasma from the core to the wall. Due to the presence of spatially localized sinks and sources, the PV profile is expected to be non-constant. Nonetheless, we speculate that the plasma can be organized such that the Lagrangian invariants are constant in bounded regions. A stepwise homogenization has been observed in geophysical [6, 7] and astrophysical [3] systems, where strong zonal flows near the interfaces between the regions of constant PV have been observed. We hypothesize that similar mechanisms involving homogenization of PV could be relevant for explaining the large scale flows associated with transport barriers in magnetically confined plasmas.

In order to illustrate this hypothesis, we have inferred the ion temperature and the electric field profiles by solving the coupled boundary value problems in equations (30) and (32) for given profiles of the particle density $n_i(x)$, the magnetic field $B(x)$ and the TEP constants $c_1(x)$ and $c_2(x)$. We show two examples to illustrate how the constants c_1 and c_2 influence the solutions. In both examples the particle density profile is a monotonically decreasing function with a localized steep gradient pedestal region. The boundary value problems were solved numerically using the **bvp4c** Matlab routine [29]. All quantities are Bohm normalized:

$$x/\rho_{i0} \to x, \quad \tau\Omega_{i0} \to \tau, \quad e\phi/t_{i0} \to \phi, \quad t_{i\perp}/t_{i0} \to t_{i\perp}, \\ n_i/n_{i0} \to n_i \quad (37)$$

where $t_{i0} = t_{i\perp}(x = 0)$, Ω_{i0} is the ion gyro-frequency at $x = 0$ and $\rho_{i0} = \Omega_{i0}^{-1}\sqrt{t_{i0}/m_i}$. In both examples the equations were solved on a domain $0 \leqslant x \leqslant 100$ and we applied the boundary conditions

$$t_{i\perp}(0) = 1, \quad \frac{\mathrm{d}}{\mathrm{d}x}t_{i\perp}(100) = 0, \quad \phi(0) = \phi(100) = 0. \quad (38)$$

5.1. Example 1: stepwise homogenization

As shown in figure 1 the particle density is proportional to the magnetic field except near $x = 50$, where the value of the particle density strongly decreases. c_1 and c_2 are chosen such that they follow the background value of the $N \propto B$ TEP state defined in equation (30) where $\omega^* \simeq 0$. Since n_i is proportional to B away from $x = 50$ we get that $c_1(x) = c_2(x) = n_i(x)/B(x)$. As shown in figure 1(a), c_1 and c_2 are therefore stepwise constant. The solutions $t_{i\perp}$ and ϕ are shown in figures 1(a) and (b), respectively. Outside the steep gradient region the ion temperature coincides with the particle density profile and is therefore proportional to the magnetic field. Also, the electric field goes towards zero outside the steep region. Since $n_i \propto B$ in these regions it is not surprising that t_i and ϕ are solutions to equations (33)–(34). Near $x = 50$ we observe that the ion temperature strongly decreases as has a negative slope comparable to the particle density gradient but slightly less steep. The electric field is negative and is strongly sheared forming a well centered around $x \simeq 50$.
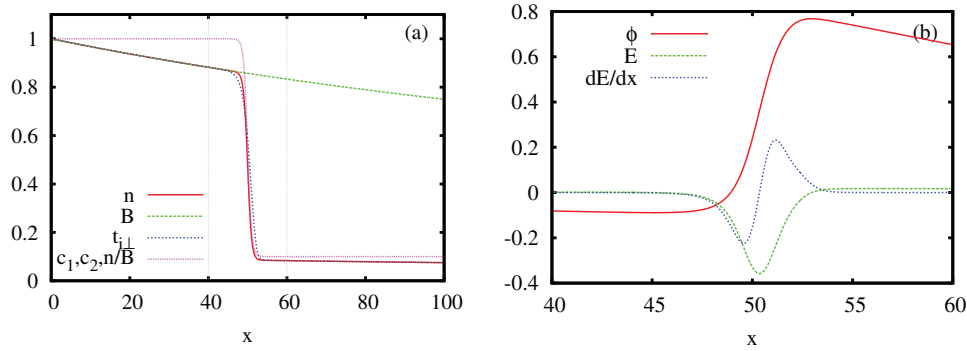
Figure 1. Input profiles of (*a*) particle density *n*, magnetic field strength *B*, TEP states c_1 and c_2 and *n/B*. Vertical grey lines indicate the domain plotted in (*b*). Numerical solutions to the coupled boundary value problems given in equations (30) and (32) for (*a*) $t_{i\perp}$ and (*b*) the electric potential ϕ, also showing the electric field *E* and the shearing rate d*E*/d*x*.
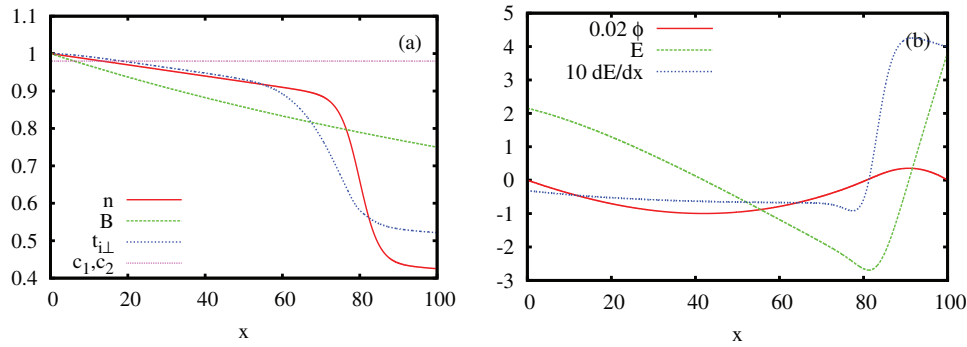

Figure 2. Input profiles of (*a*) particle density *n*, magnetic field strength *B* and TEP states c_1 and c_2. Numerical solutions to the coupled boundary value problems given in equations (30) and (32) for (*a*) $t_{i\perp}$ and (*b*) the electric potential ϕ, also showing the electric field *E* and the shearing rate d*E*/d*x*.

5.2. Example 2: TEP state with particle density pedestal

Another possible scenario is that profiles are driven towards the TEP states given in equations (30) and (32) across a particle density pedestal region. In this case the TEP state constants are fixed to the mean value of *n/B*: $c_1 = c_2 = 0.98$. The solutions $t_{i\perp}$ and ϕ to the coupled boundary value problems given in equations (30) and (32) are shown in figures 2(*a*) and (*b*), respectively. The ion temperature profile decreases in the vicinity of the particle density pedestal region, but the ion temperature profile is less steep than the particle density profile. In the region to the left of the particle density pedestal region the electric field is approximately a linearly decreasing function and hence with a constant shearing rate. When approaching the pedestal region the electric field rapidly increases and forms a well with a strong shear. We note that these features in ion temperature and electric field profiles are qualitatively in agreement with experimental observations of sheared flows associated with transport barriers [30].

Another possible scenario is the combined ion and electron TEP state given in equation (36). In this state the ***E*** × ***B***-shearing rate is constant. Regions with constant shearing rates on each side of a transport barrier were observed in the H-1 device [31]. In future work we will compare our findings with numerical simulations and experimental measurements.

6. Summary

We have derived a non-zero ion temperature potential vorticity equation analogous to Ertel's theorem for a plasma in a 2D slab. The potential vorticity equation (14) is derived from an electrostatic, inviscid, full-F gyrofluid turbulence model, which is fully non-linear and makes no distinction between fluctuations and profiles. We show that when evaluated in the long wave-length limit the potential vorticity equals the ratio of the ion gyro-frequency plus the ***E*** × ***B*** and diamagnetic polarization densities to the particle density. We show that the gyrofluid model possesses two Lagrangian invariants which are used to derive two turbulent equipartition states given in equation (29). In the turbulent equiparition state profiles are driven towards constant potential vorticity. The turbulent equipartition states are evaluated in the long wave-length limit revealing that the turbulent equiparition states couple particle density, temperature and the electric field. We hypothesize that the results are important for zonal flows and the associated transport barriers in magnetically confined plasmas, drawing analogies to potential vorticity staircases in geophysical and astrophysical fluid dynamics. To support this hypothesis we infer the ion temperature and electric potential profiles from the turbulent equiparition states given profiles of the particle density and the magnetic field. The inferred electric field, shown in figures 1 and 2, is strongly sheared and forms a well

in regions where the particle density profiles has steep gradients and hence qualitatively share features with the observed electric field associated with transport barrier in magnetically confined plasmas.

Acknowledgments

References

[1] Ertel H 1942 *Meteorol. Z.* **59** 277
[2] Pedlosky J 1987 *Geophysical Fluid Dynamics* (New York: Springer)
[3] Marcus P and Shetty S 2011 *Phil. Trans. R. Soc.* A **369** 771
[4] Weiland J 2000 *Collective Modes in Inhomogeneous Plasma: Kinetic and Advanced Fluid Theory* (*Plasma Physics Series*) (Philadelphia: Institute of Physics)
[5] Horton C W and Ichikawa Y H 1996 *Chaos and Structures in Nonlinear Plasmas* (Singapore: World Scientific)
[6] Phillips O M 1972 *Deep-Sea Res.* **19** 797
[7] Rhines O M and Young W R 1982 *J. Fluid Mech.* **122** 347
[8] Dritschel D G and McIntyre M E 2008 *J. Atmos. Sci.* **65** 855
[9] Yankov V V 1994 *JETP Lett.* **60** 171
[10] Isichenko M B and Yankov V V 1997 *Phys. Rep.* **283** 161
[11] Yankov V V and Nycander J 1997 *Phys. Plasmas* **4** 2907
[12] Naulin V, Nycander J and Juul R J 1998 *Phys. Rev. Lett.* **81** 4148
[13] Naulin V, Juul R J and Nycander J 2003 *Phys. Plasmas* **10** 1075
[14] Garbet X *et al* 2003 *Phys. Rev. Lett.* **91** 035001
[15] Hahm T S *et al* 2008 *Phys. Plasmas* **15** 055902
[16] McDevitt C J *et al* 2010 *Phys. Plasmas* **17** 112509
[17] Madsen J 2013 *Phys. Plasmas* **20** 072301
[18] Brizard A J and Hahm T S 2007 *Rev. Mod. Phys.* **79** 421
[19] Zeiler A *et al* 1997 *Phys. Plasmas* **4** 2134
[20] Smolyakov A I 1998 *Can. J. Phys.* **76** 321
[21] Hinton F L and Horton C W 1971 *Phys. Fluids* **14** 116
[22] Chang Z and Callen J D 1992 *Phys. Fluids* B **4** 1766
[23] Brizard A 1992 *Phys. Fluids* B **4** 1213
[24] Scott B D 2007 *Phys. Plasmas* **14** 102318
[25] Wiesenberger M, Madsen J and Kendl A 2014 *Phys. Plasmas* **21** 092301
[26] Madsen J *et al* 2011 *Phys. Plasmas* **18** 112504
[27] Nycander J and Yankov V V 1996 *Phys. Scr.* T **63** 174
[28] Isichenko M B and Petviashvili N V 1995 *Phys. Plasmas* **2** 3650
[29] MATLAB 2014a (8.3.0.532), The MathWorks, Inc., Natick, Massachusetts, USA
[30] Viezzer E *et al* 2013 *Nucl. Fusion* **53** 053005
[31] Xia H *et al* 2006 *Phys. Rev. Lett.* **97** 255003